

Low Computational Complexity Control of a Three-Phases Open-Windings AC Brushless Motor

Alberto Cologni, Mirko Mazzoleni, Fabio Previdi

Dipartimento di Ingegneria Gestionale,
dell'Informazione e della Produzione
Universita' degli Studi di Bergamo
24044 Dalmine (BG), Italy
Email: alberto.cologni@unibg.it

Abstract—The computational complexity of a modulating control is always one of the biggest limitation in the real control of brushless motor. This paper presents a low computational complexity control for a three phases open-windings AC brushless motor. The control strategy is based on a modified version of the D-Q frame: this solution allows to exploit the motor control libraries, already available on some motor control microprocessors. The PWM is generated in accordance to a novel algorithm based on a combination of two standard SVM algorithms, one for each inverter.

The current controller has been tested on a real open-windings motor, installed as an active vibrations damper for aerospace applications. The experiments demonstrate the good quality of the current tracking and the high efficiency of the inverter, controlled with the proposed approach.

Index Terms—Current control, Brushless motor, Open windings, High efficiency inverter, Space vector pulse width modulation

I. INTRODUCTION

Nowadays, the need of more powerful, lightest and safer motors is become one of the most important request of the industry. In this context, the introduction of the open-winding technology for the brushless motors, allowed to increase the power-weight ratio, the reliability and to reduce the energy consumption [1].

This evolution, allowed to start a research branch in this motor architecture. Most of the early works are focused on the fault-tolerant capabilities [2], [3]. Further research activities demonstrate the power increase with the same switch rating of the components, compared with standard closed-windings motors [4]. The last activities on this topic are related to the comparison, in terms of efficiency, of different control approaches [5].

Comparing the standard star-connected motor with the open-windings one, it is easy to understand that the actuation approach must be redefined. During the last decade some control solutions have been proposed [6]–[8]. Considering one of the first research activities in this context [9] (with the introduction of a two stages actuation system), the possible

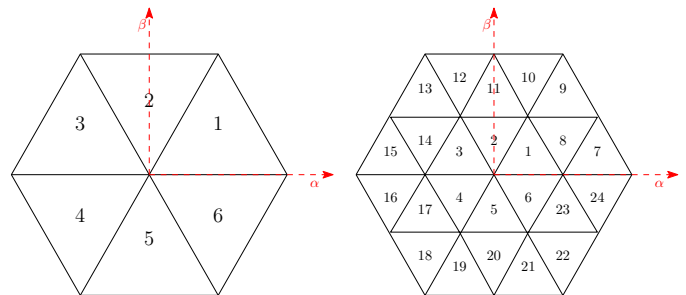


Fig. 1. SVM Actuation sectors in the star-windings (left) and open-windings (right) motors

configurations of the two inverters lead to a total number of 64 combinations of the switches. This huge number of possible conditions, implies an increase of the instructions in the SVM (Space Vector Modulation) code. In Figure 1 the SVM sectors are represented in both cases (star-windings and open-windings): the identification of the sector with the dual inverter configuration causes a significant rise of the computational effort on the micro-controller.

In this paper, a novel control algorithm for the open-windings AC brushless motor is proposed. Specifically, the first contribution of this document is to describe a low computational complexity control of a three-phases open-windings AC brushless motor. The main idea behind this technique is to guarantee balanced currents during the actuation: driving the two inverters in a certain way, also without an high complexity, it is possible to obtain symmetric currents in the windings.

A second contribution of the paper is the implementation of the designed algorithm for the control of a real motor. This activity allowed to experimentally verify the efficiency of the proposed solution. The considered case study is an active vibration damper for aerospace applications [10].

The use of active damping allows to introduce energy into the system and accurately and effectively achieve the designed performance by means of control systems [11]–[14]. An active

damping system requires sensors, actuators, a source of power and an electronic control system. The use of active damping strategies can provide fine frequency tuning, also varying with time, higher control action intensity, control of power efficiency and greater accuracy in tracking [15]. Moreover, in aerospace applications the actuator must also have small weight and high reliability (see [16] as an example). In particular, active vibration damping systems based on Electro-Mechanical Actuators (EMAs) have been already successfully used, especially in those applications where high force values at quite low frequency are necessary (see [17] as an example).

The use of this type of motors allows to optimize some of the critical limits of the application of electro-mechanical actuator in the aerospace field. It allows to:

- increase the power-weight ratio;
- increase the maximum current, and consequently the torque, with a certain DC bus voltage;
- increase the reliability of the actuation system thanks to the fault-tolerant structure of the open-windings motor

In this context, the design, the implementation and the testing of a new control solution for an innovative actuation system allows to move forward the research limit.

The remainder of the paper is as follows. In Section II, the control approach for the open-windings AC brushless motor is detailed. In Section III the layout of the experimental setup is described, and a description of the experiments has been carried out. Section IV is devoted to the results description and analysis. Some concluding remarks end the paper.

II. PROPOSED APPROACH

The motor control requires to actuate a set of output that determine the voltages of the motor windings. In this section, the control algorithms necessary for this purpose are described.

A. Control of a star-windings motor

Considering the classic star-windings motor, the defined voltages are three (one for each phase), usually actuated using the PWM (Pulse-Width Modulation).

In Figure 2 it is possible to observe the input signals necessary to drive the motor. The signals are, generally, two for each terminal: one that commands the upper mosfet (connected to the positive line of the DC bus) and the other one that commands the lower one (connected to the ground of the DC bus). Considering, however, the structure of the circuit, it is easy to understand that, the upper command (e.g $P_{a,h}^+$) and the lower one on the same leg ($P_{a,l}^+$) can't be activated simultaneously; for this reason it is possible to consider the signals as one for each winding (the two commands are one the negate of the other, neglecting the dead time necessary for the mosfet commutation).

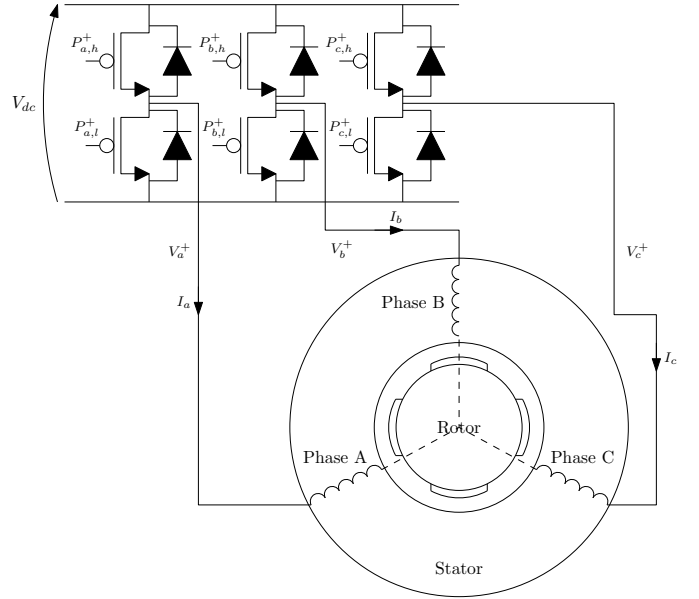


Fig. 2. Structure of a single inverter

In the star-windings case, using Kirkoff, it is possible to write the simple current balance:

$$I_a + I_b + I_c = 0 \quad (1)$$

It means that, in order to control a star-windings motor it is necessary to acquire two of the three currents. Once extracted (by means of measure or calculus) the three currents, it is possible to obtain, using the Clarke transformation, the two currents I_α and I_β that represent the current component in the direction of the first winding, and the perpendicular one (both integral with the stator).

$$I_{\alpha,\beta,\gamma} = \frac{2}{3} \begin{bmatrix} 1 & -\frac{1}{2} & -\frac{1}{2} \\ 0 & \frac{\sqrt{3}}{2} & -\frac{\sqrt{3}}{2} \\ \frac{1}{2} & \frac{1}{2} & \frac{1}{2} \end{bmatrix} \begin{bmatrix} I_a \\ I_b \\ I_c \end{bmatrix} \quad (2)$$

Combining the equations 1 and 2 it is easy to calculate the value of I_γ : it is always zero (the currents are automatically balanced).

Using the Park transformation, it is possible to obtain the quadrature current I_q and the direct current I_d : these currents depend from the rotor position θ and represent, respectively, the motor torque and the power losses (I_γ doesn't change because it represents the current on the rotation axis).

$$I_{d,q,\gamma} = \begin{bmatrix} \cos(\theta) & \sin(\theta) & 0 \\ -\sin(\theta) & \cos(\theta) & 0 \\ 0 & 0 & 1 \end{bmatrix} \begin{bmatrix} I_\alpha \\ I_\beta \\ I_\gamma \end{bmatrix} \quad (3)$$

Once obtained the d-q measures, it is possible to close two control loops, in order to provide the defined voltages to the motor.

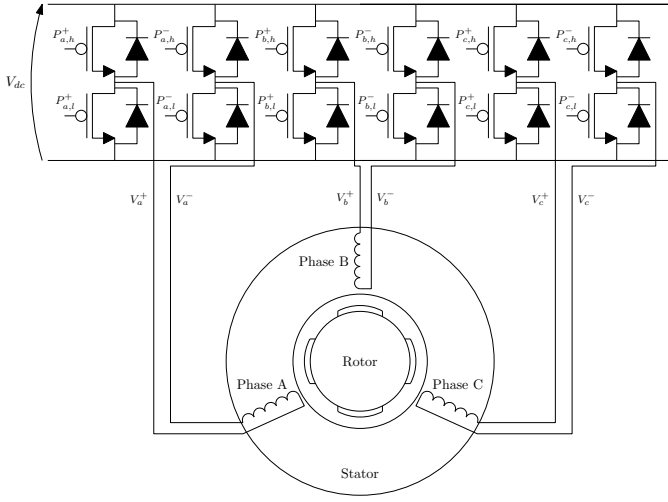


Fig. 3. Structure of a dual inverter

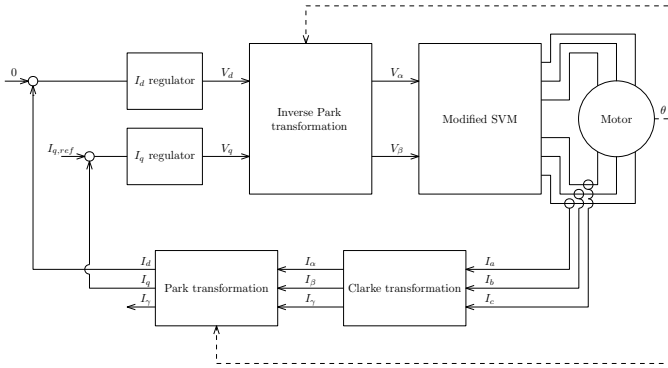


Fig. 4. Structure of the open-windings control

B. Control of a open-windings motor

Considering an open-windings motor (the structure of which is depicted in Figure 3), it is easy to understand that the actuation algorithm must be redesigned, in order to manage the number of output to the motor (6 voltages instead of 3).

The control techniques for this type of motors, are based on the scheme represented in Figure 4. The layout is similar to that used in the star-windings motors: starting from the current measures (in this case of the three windings, because Equation 1 is not valid), it is possible to extract, using Clark and Park transformation, the I_d and I_q measures, and, using two control loops, the two (direct and quadrature) voltages can be defined. The stator currents, extracted through the inverse Park transformation, enter in the SVM module, that determines the six PWM to the windings.

The SVM calculus is the completely redesigned part in respect to the star-windings motor. Considering the classical two-levels approach, the number of possible switches in function of the active sector is 24. This huge number of conditions implies an increase of the computation needed to define the

PWM values for each cycle.

The proposed approach is based on this concept: exploit the standard SVM algorithm in order to extend the number of outputs, guaranteeing an high efficiency (low I_d and I_γ). In order to guarantee the balance of the currents in the windings ($I_\gamma = 0$), the concept is to feed a second standard SVM using the negate V_α and V_β signals.

Modified SVM

- A. **Standard SVM:** execute the standard SVM with the inputs V_α and V_β .
- B. **Calculate the opposite stator voltages:** compute the two opposite stator voltages $V_{\alpha,neg} = -V_\alpha$ and $V_{\beta,neg} = -V_\beta$.
- C. **Opposite SVM:** execute the standard SVM with the inputs $V_{\alpha,neg}$ and $V_{\beta,neg}$.
- D. **Assign outputs:** assign the output of the standard SVM to the first inverter and the outputs of the opposite SVM to the lower one.

The details of the algorithm are defined in Table I, where ϕ represents the angle formed by the V_α and V_β components in the $V_\alpha - V_\beta$ space with respect to the V_α axis.

In order to evaluate the performance of this approach, a real experiment is carried out, and an efficiency analysis is presented.

III. EXPERIMENTAL SETUP

The low complexity control has been implemented on a real actuator, in order to verify its performance.

The actuator has been designed for the use in a classic layout for dynamic vibration damping. The damper is connected to an un-damped main mass-spring system, and tuned to the resonant frequency of the main mass-spring. When a force, with the same frequency of the tuned resonant frequency of the damping system, is applied, there is no motion of the main mass, and no net reaction force (other than static equilibrium force) is required at the mechanical constraint. This can be achieved by measuring the vibration force and applying the correct counteracting force with the actuator (see Figure 5).

The system can be described by the equations of motion of a lumped parameter model (see Figure 6). The ballscrew joint can be assumed to be an infinite wedge with angle α :

$$\begin{aligned}
 M\ddot{x}_m &= k_s(x_i - x_M) + k_{eq}(x_v + y_v \tan(\alpha) - x_M) + \\
 &+ c_s(\dot{x}_i - \dot{x}_M) + c_c(\dot{x}_v + \dot{y}_v \tan(\alpha) - \dot{x}_M) \quad (4) \\
 m_v\ddot{x}_v &= k_v(x_i - x_v) - k_{eq}(x_v + y_v \tan(\alpha) - x_M) + \\
 &+ c_v(\dot{x}_i - \dot{x}_v) - c_c(\dot{x}_v + \dot{y}_v \tan(\alpha) - \dot{x}_M) \quad (5) \\
 m_{eq}\ddot{y}_v \tan(\alpha) &= -k_{eq}(x_v + y_v \tan(\alpha) - x_M) + \\
 &- c_c(\dot{x}_v + \dot{y}_v \tan(\alpha) - \dot{x}_M) \quad (6)
 \end{aligned}$$

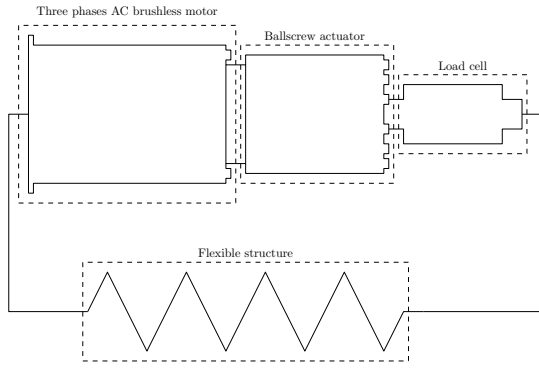


Fig. 5. Actuator scheme

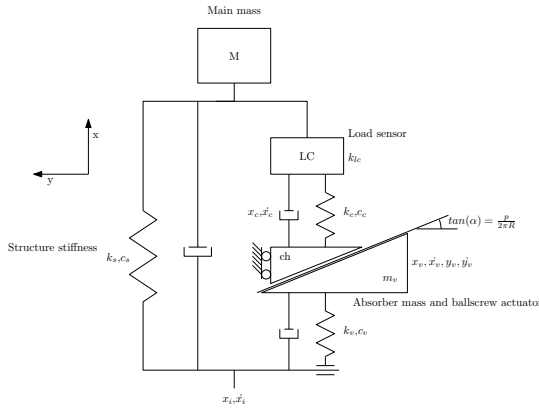


Fig. 6. Mechanical model of the actuator

where:

- M is the main mass;
- m_v is the mass of the actuator;
- k_s and c_s are respectively the elastic constant and the damping coefficient of the load spring;
- k_c and c_c are respectively the elastic constant and the damping coefficient of the load sensor;
- k_v and c_v are respectively the elastic constant and the damping coefficient of the connection between the sensor and the actuator;
- k_{lc} is the elastic constant of the load sensor;
- $k_{eq} = \frac{k_c k_{lc}}{k_c + k_{lc}}$ is the equivalent elasticity of the load sensor and its connection to the actuator.

All the mechanical structures are designed in order to have parameters (masses, stiffness and damping) as close as possible aligned to the required resonance (25 Hz).

The electronic layout is based on a freescale micro-controller (DSP 56800). The technical details are the following:

- Three phases motor with sinusoidal BEMF;
- DC bus at 28 V;
- nominal power of 750 W;
- two three phases bridges with 100 A of maximum current;

- high dynamic current sensors with a range of ± 100 A

The control system for the presented activity is based on two nested control loops. The inner one is the current control systems (the core of the publication); while the second one is a force controller.

This actuator is designed in order to work in a defined frequency (in particular the resonance frequency of the spring-mass structure). For this reason, the tests (described in Section IV) are executed with a reference sinusoidal signal at 25 Hz.

IV. RESULTS

The experiments of the real system allow to analyze the performance of the proposed approach.

During the tests a certain I_q reference is defined (as already discussed a sine at 25 Hz), while a zero reference is selected for I_d . Once obtained the measures on the real system (I_d , I_q and I_γ) it is possible to calculate the efficiency of the inverter [18].

The actuator has been tested on a test bench with an elastic load. The actuator performance have been assessed in experiments at the target working frequency f_w , by measuring the generated force, the kinematic parameters (angular and linear displacement/velocity/acceleration) and current/power absorption.

The tested I_q reference is a sine with an amplitude of 10 A and a frequency of 25 Hz. The performance of the control loop are depicted in Figure 7: the quality of the tracking is good; the RMSEs (Root Mean Square Errors) are the followings:

- I_q : 0.8 A;
- I_d : 0.738 A;
- I_γ : 1.092 A.

In order to evaluate the performance it is necessary to calculate the overall efficiency of the control. Starting from the I_d , I_q and I_γ , the overall efficiency can be calculated as:

$$\eta(t)[\%] = 100 \frac{\sqrt{I_q(t)^2}}{\sqrt{I_d(t)^2 + I_q(t)^2 + I_\gamma(t)^2}} \quad (7)$$

The result of this calculus are depicted in Figure 8: the average efficiency is 92 % (with the sinusoidal I_q reference).

Another important result of the introduction of this open-windings architecture, is the possibility of increase the reliability of the motor: with this configuration, the motor is able to actuate (in each rotor position) also disabling one of the three phases.

In order to verify the performance in these conditions, a test has been performed, disconnecting one of the motor phases (simulating a failure on a winding or on a component of the three phases bridge). The results of this experiment are depicted in Figure 9; the RMSEs are, in this case, the followings:

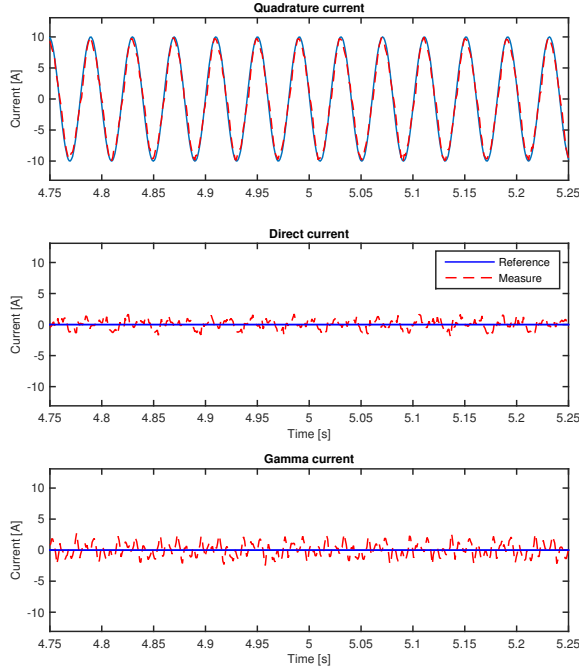


Fig. 7. Control performance in the nominal conditions

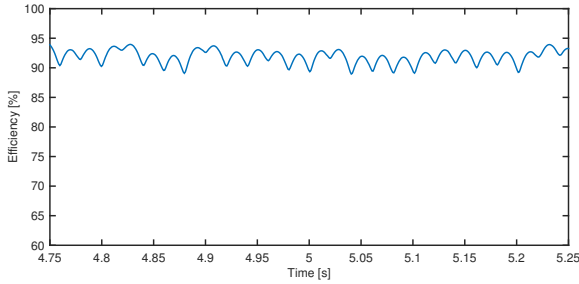


Fig. 8. Control efficiency in the nominal conditions

- I_q : 1.248 A;
- I_d : 1.55 A;
- I_γ : 3.604 A.

The overall efficiency, in case of one phase fault, is represented in Figure 10: the average efficiency is 81.8 %.

V. CONCLUSIONS

In this paper, a low-computational complexity algorithm, for the control of a three-phases open-windings AC brushless motor has been proposed. The main idea is to exploit the standard Space Vector Modulation in order to calculate the command signals to the lower bridge, using a modification of the inputs of this algorithm. In this way, the complexity of the calculus is reduced, comparing to the common multi-levels open-windings control architectures [4]. The approach

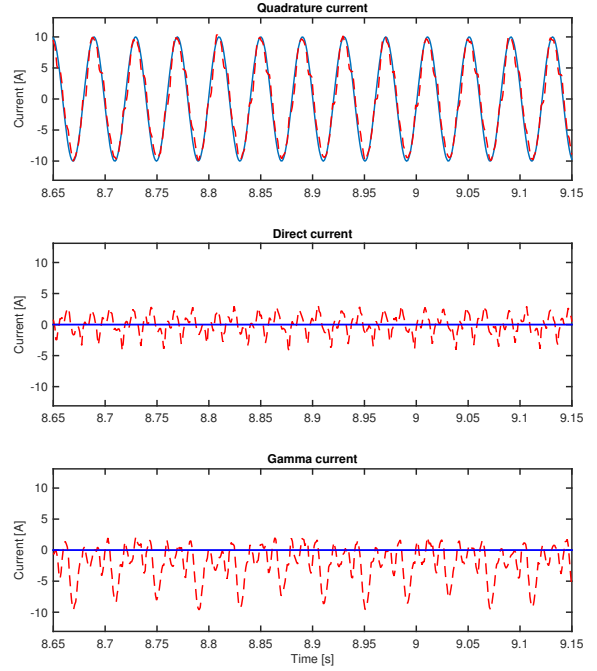


Fig. 9. Control performance with a phase fault

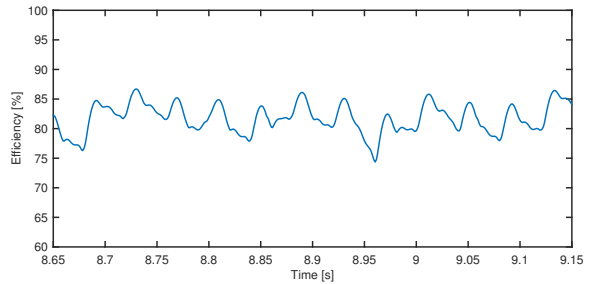


Fig. 10. Control efficiency with a phase fault

has been first presented qualitatively and then discussed in detail on an experimental case study.

Specifically, the control of an active damper for an aerospace application has been coped with and satisfactory results have been obtained. From a practical point of view, the control performance denote a very high efficiency of the inverter (92 %) and the possibility of work with only two phases with an acceptable efficiency (81.8 %).

Future work will be devoted to the optimization of the efficiency in case of failure, switching the SVM to another modified version.

REFERENCES

- [1] V. T. Somasekhar, K. Gopakumar, M. Baiju, K. K. Mohapatra, and L. Umanand, "A multilevel inverter system for an induction motor with open-end windings," *Industrial Electronics, IEEE Transactions on*, vol. 52, no. 3, pp. 824–836, 2005.
- [2] T. M. Jahns, "Improved reliability in solid-state ac drives by means of multiple independent phase drive units," *Industry Applications, IEEE Transactions on*, no. 3, pp. 321–331, 1980.
- [3] B. Mecrow, A. Jack, J. Haylock, and J. Coles, "Fault-tolerant permanent magnet machine drives," *IEE Proceedings-Electric Power Applications*, vol. 143, no. 6, pp. 437–442, 1996.
- [4] B. Welchko, J. M. Nagashima *et al.*, "The influence of topology selection on the design of ev/hev propulsion systems," *Power Electronics Letters, IEEE*, vol. 1, no. 2, pp. 36–40, 2003.
- [5] P. Sandulescu, F. Meinguet, X. Kestelyn, E. Semail, and A. Bruyere, "Control strategies for open-end winding drives operating in the flux-weakening region," *Power Electronics, IEEE Transactions on*, vol. 29, no. 9, pp. 4829–4842, 2014.
- [6] Y. Kawabata, M. Nasu, T. Nomoto, E. C. Ejiogu, and T. Kawabata, "High-efficiency and low acoustic noise drive system using open-winding ac motor and two space-vector-modulated inverters," *Industrial Electronics, IEEE Transactions on*, vol. 49, no. 4, pp. 783–789, 2002.
- [7] A. K. Gupta and A. M. Khambadkone, "A space vector pwm scheme for multilevel inverters based on two-level space vector pwm," *Industrial Electronics, IEEE Transactions on*, vol. 53, no. 5, pp. 1631–1639, 2006.
- [8] H. Nian and Y. Zhou, "Investigation of open-winding pmsg system with the integration of fully controlled and uncontrolled converter," *Industry Applications, IEEE Transactions on*, vol. 51, no. 1, pp. 429–439, 2015.
- [9] E. Shivakumar, K. Gopakumar, S. Sinha, A. Pittet, and V. Ranganathan, "Space vector pwm control of dual inverter fed open-end winding induction motor drive," in *Applied Power Electronics Conference and Exposition, 2001. APEC 2001. Sixteenth Annual IEEE*, vol. 1. IEEE, 2001, pp. 399–405.
- [10] F. Previdi, A. Cologni, M. Madaschi, N. Matteuzzi, M. Nardeschi, S. Toro, and S. M. Savaresi, "Modeling and control of an electro-mechanical ballscrew actuator for vibration active damping," in *Control Applications (CCA), 2014 IEEE Conference on*. IEEE, 2014, pp. 177–182.
- [11] M. J. Balas, "Feedback control of flexible systems," *Automatic Control, IEEE Transactions on*, vol. 23, no. 4, pp. 673–679, 1978.
- [12] J. J. Dosch, D. J. Inman, and E. Garcia, "A self-sensing piezoelectric actuator for collocated control," *Journal of Intelligent Material Systems and Structures*, vol. 3, no. 1, pp. 166–185, 1992.
- [13] J. M. Goodliffe, "Self-sensing piezoelectric actuation: analysis and application to controlled structures," 1992.
- [14] P. Vallone, "High-performance piezo-based self-sensor for structural vibration control," in *Smart Structures & Materials' 95*. International Society for Optics and Photonics, 1995, pp. 643–655.
- [15] F. Previdi, C. Spelta, M. Madaschi, D. Belloli, S. M. Savaresi, F. Fagnoli, and E. Silani, "Active vibration control over the flexible structure of a kitchen hood," *Mechatronics*, vol. 24, no. 3, pp. 198–208, 2014.
- [16] A. Garcia, J. Rosero, J. Ortega, L. Romeral *et al.*, "Reliable electro-mechanical actuators in aircraft," *Aerospace and Electronic Systems Magazine, IEEE*, vol. 23, no. 8, pp. 19–25, 2008.
- [17] K. Nakano, Y. Suda, and S. Nakadai, "Self-powered active vibration control using a single electric actuator," *Journal of Sound and Vibration*, vol. 260, no. 2, pp. 213–235, 2003.
- [18] E. Shivakumar, V. Somasekhar, K. K. Mohapatra, K. Gopakumar, L. Umanand, and S. Sinha, "A multi level space phasor based pwm strategy for an open-end winding induction motor drive using two inverters with different dc link voltages," in *Power Electronics and Drive Systems, 2001. Proceedings., 2001 4th IEEE International Conference on*, vol. 1. IEEE, 2001, pp. 169–175.

TABLE I
DUAL-INVERTER SVM ALGORITHM

(a)	
ϕ	High bridge (+)
$[0, \pi/3)$	$V_a^+ = \frac{\sqrt{3}}{2} V_\alpha + \frac{1}{2} V_\beta + 1$ $V_b^+ = \frac{-\sqrt{3}}{2} V_\alpha + \frac{3}{2} V_\beta + 1$ $V_c^+ = \frac{-\sqrt{3}}{2} V_\alpha - \frac{1}{2} V_\beta + 1$
$[\pi/3, 2/3\pi)$	$V_a^+ = \frac{\sqrt{3}}{2} V_\alpha + \frac{1}{2}$ $V_b^+ = \frac{1}{2} V_\beta + \frac{1}{2}$ $V_c^+ = -\frac{1}{2} V_\beta + \frac{1}{2}$
$[2/3\pi, \pi)$	$V_a^+ = \frac{\sqrt{3}}{2} V_\alpha - \frac{1}{2} V_\beta + 1$ $V_b^+ = \frac{-\sqrt{3}}{2} V_\alpha + \frac{3}{2} V_\beta + 1$ $V_c^+ = \frac{-\sqrt{3}}{2} V_\alpha - \frac{1}{2} V_\beta + 1$
$[\pi, 4/3\pi)$	$V_a^+ = \frac{\sqrt{3}}{2} V_\alpha + \frac{1}{2} V_\beta + 1$ $V_b^+ = \frac{-\sqrt{3}}{2} V_\alpha + \frac{3}{2} V_\beta + 1$ $V_c^+ = \frac{-\sqrt{3}}{2} V_\alpha - \frac{1}{2} V_\beta + 1$
$[4/3\pi, 5/3\pi)$	$V_a^+ = \frac{\sqrt{3}}{2} V_\alpha + \frac{1}{2}$ $V_b^+ = \frac{1}{2} V_\beta + \frac{1}{2}$ $V_c^+ = -\frac{1}{2} V_\beta + \frac{1}{2}$
$[5/3\pi, 2\pi)$	$V_a^+ = \frac{\sqrt{3}}{2} V_\alpha - \frac{1}{2} V_\beta + 1$ $V_b^+ = \frac{-\sqrt{3}}{2} V_\alpha + \frac{3}{2} V_\beta + 1$ $V_c^+ = \frac{-\sqrt{3}}{2} V_\alpha - \frac{1}{2} V_\beta + 1$
(b)	
ϕ	Low bridge (-)
$[0, \pi/3)$	$V_a^- = \frac{-\sqrt{3}}{2} V_\alpha - \frac{1}{2} V_\beta + 1$ $V_b^- = \frac{\sqrt{3}}{2} V_\alpha - \frac{3}{2} V_\beta + 1$ $V_c^- = \frac{\sqrt{3}}{2} V_\alpha + \frac{1}{2} V_\beta + 1$
$[\pi/3, 2/3\pi)$	$V_a^- = -\frac{\sqrt{3}}{2} V_\alpha + \frac{1}{2}$ $V_b^- = -\frac{1}{2} V_\beta + \frac{1}{2}$ $V_c^- = \frac{1}{2} V_\beta + \frac{1}{2}$
$[2/3\pi, \pi)$	$V_a^- = \frac{-\sqrt{3}}{2} V_\alpha + \frac{1}{2} V_\beta + 1$ $V_b^- = \frac{\sqrt{3}}{2} V_\alpha - \frac{3}{2} V_\beta + 1$ $V_c^- = \frac{\sqrt{3}}{2} V_\alpha + \frac{1}{2} V_\beta + 1$
$[\pi, 4/3\pi)$	$V_a^- = \frac{-\sqrt{3}}{2} V_\alpha - \frac{1}{2} V_\beta + 1$ $V_b^- = \frac{\sqrt{3}}{2} V_\alpha - \frac{3}{2} V_\beta + 1$ $V_c^- = \frac{\sqrt{3}}{2} V_\alpha + \frac{1}{2} V_\beta + 1$
$[4/3\pi, 5/3\pi)$	$V_a^- = -\frac{\sqrt{3}}{2} V_\alpha + \frac{1}{2}$ $V_b^- = -\frac{1}{2} V_\beta + \frac{1}{2}$ $V_c^- = \frac{1}{2} V_\beta + \frac{1}{2}$
$[5/3\pi, 2\pi)$	$V_a^- = \frac{-\sqrt{3}}{2} V_\alpha + \frac{1}{2} V_\beta + 1$ $V_b^- = \frac{\sqrt{3}}{2} V_\alpha - \frac{3}{2} V_\beta + 1$ $V_c^- = \frac{\sqrt{3}}{2} V_\alpha + \frac{1}{2} V_\beta + 1$